Fuel 348 (2023) 128302

Contents lists available at ScienceDirect

Fuel

journal homepage: www.elsevier.com/locate/fuel

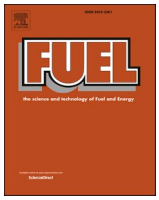

Full Length Article

High pressure ammonia oxidation in a flow reactor

P. García-Ruiz, M. Uruén, M. Abián, M.U. Alzueta *

Aragón Institute of Engineering Research (I3A), Department of Chemical and Environmental Engineering, University of Zaragoza, 50018 Zaragoza, Spain

ARTICLE INFO

Keywords:
Ammonia
NH_3
High pressure
Kinetic modeling
Oxidation
NO

ABSTRACT

The present work deals with an experimental and modeling analysis of ammonia oxidation at high pressure (up to 40 bar), in the 600–1275 K temperature range using a quartz tubular reactor and argon as diluent. The impact of temperature, pressure, oxygen stoichiometry and presence of NO has been analyzed on the concentrations of NH_3 and N_2 obtained as main products of ammonia oxidation. The main results obtained indicate that increasing either pressure or stoichiometry results in a shift of NH_3 conversion to lower temperatures. The effect of pressure is particularly significant in the low range of pressures studied. The main product of ammonia oxidation is N_2, while NO, NO_2 and N_2O concentrations are below the detection limit for all the conditions considered. The experimental results are simulated and interpreted in terms of a literature detailed chemical kinetic mechanism, which, in general, predicts satisfactorily the experimental results.

1. Introduction

Combating climate change by reducing greenhouse gas is one of the biggest challenges in the XXI century, and reducing CO_2 emissions plays a determining role. For this reason, clean and renewable fuels are important for future power systems. For this purpose, alternative fuels such as hydrogen and ammonia are becoming more and more important.

Hydrogen has attracted attention as a carbon-free transportation fuel with zero CO_2 emissions [e.g. 1], but its storage capability problems (very high pressures are required at room temperature), its high transportation equipment cost because of the necessity of liquefaction at low temperature (−252.9 °C, Table S1 of the supplementary material), and its low volumetric energy density represent a barrier to its implementation [2,3]. For example, in fuel cell vehicles, a 700 atm hydrogen storage tank is, at least, needed to obtain a similar range of operation to that of vehicles using gasoline or diesel fuels for a similar volume of the deposit [4].

According to the International Energy Association [5], focusing on strategies for renewable energy utilization in the industrial sector, ammonia is mentioned to be one of the most attractive energy carriers with significant economic advantages [4].

Ammonia is a potential carbon-free energy carrier and a power generation compound [6,7]. Its use as an energy vector has several advantages: low cost, easy storage and transport [e.g. 2–4] with a matured infrastructure for its handling, besides being an efficient additive for Selective Non-Catalytic Reduction (SNCR) of NO in combustion processes [e.g. 8–11]. Additionally, ammonia can, ideally, be burned in an environmentally benign way producing N_2 and H_2O.

However, ammonia has also some drawbacks, when compared to common hydrocarbon fuels, such as its low combustion intensity and flammability [4], a potentially high NO_x emission, low radiation intensity and high autoignition temperature [12]. The heat of combustion of ammonia and the maximum laminar burning velocity of an NH_3/air flame are about 40% and 20%, respectively, of those for typical hydrocarbon fuels, as shown in Table S1 of the supplementary material. The ammonia/air flame temperature and radiation heat transfer from the flame are also lower than those of hydrocarbon flames [4].

Ammonia combustion at atmospheric pressure has been reported in the literature, in particular in the very recent years. Among the different studies published, we can mention works performed using laboratory reactors, such as flow reactors [e.g. 13–19], perfect stirred reactors [e.g. 16,17,20], shock tubes [e.g. 21–23], and flames [e.g. 24–30]. Also, a number of more applied studies dealing with ammonia combustion in engines and turbines can be found in the recent literature [e.g. 7,31–33]. Those studies have contributed to determine the conversion regime of ammonia under a variety of conditions, together with the contribution to the formation of pollutant emissions, namely NO. The experimental work made has been supported by different kinetic mechanisms developed for modelling the conversion of ammonia, as well as its mixtures with other fuels [e.g. 11,12,17,21,28].

Despite the various laboratory studies dealing with NH_3 conversion, investigations at high pressures (above 5 bar) are still scarce, and mainly

* Corresponding author.
E-mail address: uxue@unizar.es (M.U. Alzueta).

https://doi.org/10.1016/j.fuel.2023.128302
Received 25 January 2023; Received in revised form 30 March 2023; Accepted 31 March 2023
Available online 12 May 2023

include mixtures of ammonia with different combustibles or different reactors than the one used in the present study. Among the high pressure studies, we can mention the high pressure flow reactor study by Song et al. [15], and the high pressure studies carried out in a rapid compression machine by Dai et al. [34–36], at pressures above 20 bar. In general, the works carried out at high pressures have showed that increasing pressure restricts the production of NO in flames [26], and indicate that both the O_2 availability and the pressure have important effects on the ignition delay time of ammonia [21]. The ignition delay time was seen to decrease with increasing pressure, which in turn was attributed to the increase in absolute concentration of reactants at high pressures, which promotes the oxidation process [34–36].

To our knowledge, the only experimental results obtained at high pressures and in a plug flow reactor are those of Song et al. [15], which focused on ammonia oxidation at intermediate temperatures (up to 925 K) and at pressures of 30 and 100 bar, conditions relatively comparable to the ones considered in the present work. Song et al. [15] reported that the onset temperature of ammonia oxidation is approximately the same for both pressures (30 and 100 bar), considerably lower than the temperature at which conversion of ammonia occurs atmospheric pressure [e.g. 18]. In this context, the present work aims to extend the range of study of ammonia oxidation at intermediate pressures (from 10 to 40 bar). Filling the gap between atmospheric pressure and high pressures is of interest in order to know the effect of the pressure in the ammonia oxidation process in a wide pressure interval. The present work also extends significantly the temperature interval in which NH_3 conversion is studied compared to the Song et al. [15] study, reaching in the present experiments temperatures of up to 1275 K, which allow us to see the complete conversion of ammonia, at least in some cases. Additionally, the present experiments are performed using argon as bath gas, which allows us to determine with precision the nitrogen balance, for the different conditions considered.

Thus, apart from varying pressure in the 10 to 40 bar range, the temperature has been changed between 600 and 1275 K, and different stoichiometries, ranging from fuel-rich to fuel-lean, have been considered. Also, the presence of NO, that can be present simultaneously with ammonia within the combustion chamber, has been considered. The results have been simulated with a literature mechanism and the main reaction pathways occurring under the various conditions studied have been identified. Comparison of the results of the present work and results obtained under atmospheric pressure conditions and similar conditions [18] has also been done.

2. Methodology

Conversion of reactants and formation of products during the oxidation of NH_3 are studied under well-controlled laboratory-scale conditions at high pressure. The laboratory setup, which has been used with success in previous works where it is described in detail [e.g. 37,38], is schematized in detail in Fig. 1.

The reactant gases are fed from gas cylinders (provider: Air Liquide, Praxair or Messer) and premixed before entering the quartz flow reactor (153.8 cm long, inner diameter of 6 mm), which is placed inside a 3 zone electrically heated oven, allowing an isothermal zone inside the tube of approximately 35 cm. This isothermal zone was determined experimentally through the temperature profiles performed for different temperatures and pressures. Fig. 2 shows, as an example, the temperature profiles measured for the pressure of 40 bar, using a gas flow rate of 1000 ml (STP)/min, as has been used in all the experiments. The temperature profiles along the reactor were determined using a thermocouple positioned in the space between the quartz tube and the steel shell used to keep the pressure constant. The temperature measurement was taken each 5 cm in the central zone and each 10 cm at both sides of the reactor.

In the present work, the effect of the main variables: oxygen excess ratio (reducing $\lambda = 0.7$, stoichiometric, $\lambda = 1$, and oxidizing, $\lambda = 3$, conditions), pressure (10, 20, 30 and 40 bar) and temperature (from 600 to 1275 K) has been studied, using a nominal ammonia concentration of 1000 ppm. The oxygen excess ratio (λ) is defined according to the NH_3 oxidation reaction to N_2 (i.e·$NH_3 + 0.75\ O_2 \rightarrow 0.5\ N_2 + 1.5\ H_2O$) according to equation (1):

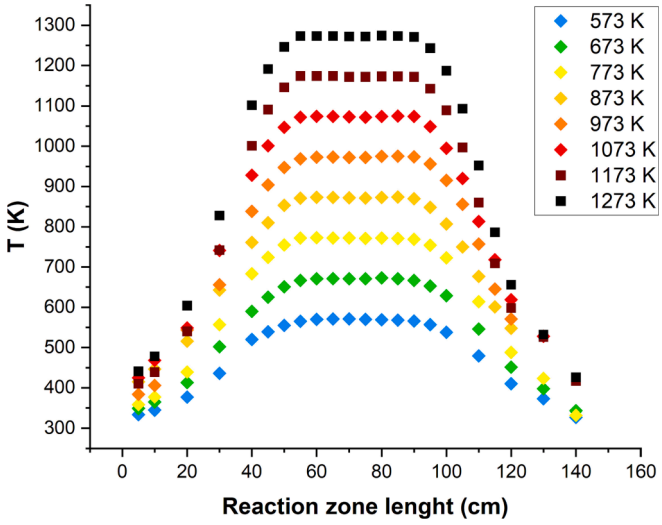

Fig. 2. Temperature profiles as a function of the reactor length at 40 bar, for different nominal temperatures.

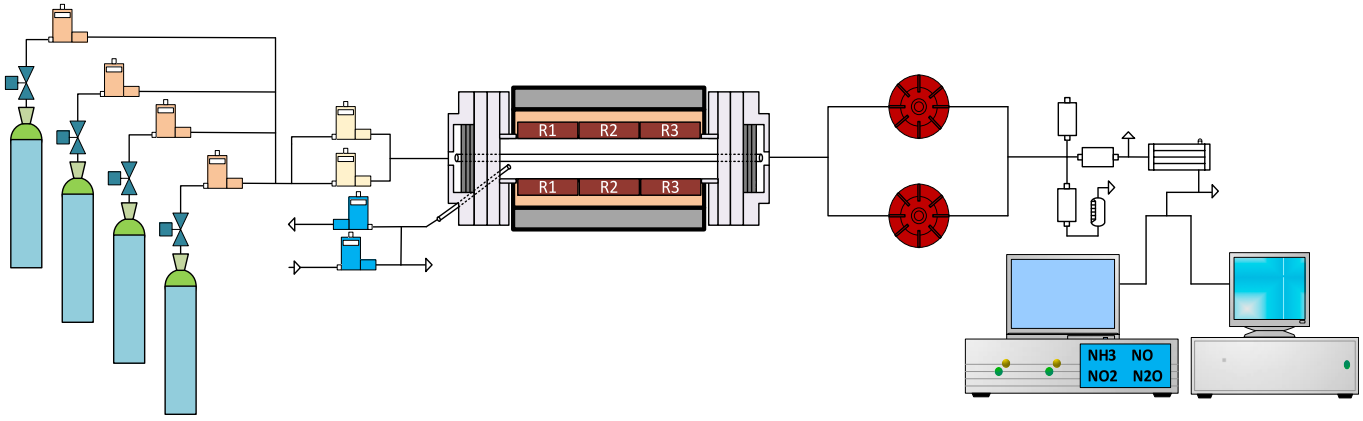

Fig. 1. Laboratory-scale high pressure setup.

$$\lambda = \frac{(O_2)_{inlet}}{(O_2)_{stoichiometric}} \quad (1)$$

In the experiments, the flow rate is 1000 ml (STP)/min, which gives a temperature and pressure dependent gas residence time in the isothermal reaction zone, as described in equation (2).

$$t_r\ (s) = 231.6 \cdot \frac{P\ (bar)}{T\ (K)} \quad (2)$$

Concentrations of NH_3, N_2, H_2, O_2, NO, NO_2 and N_2O are analyzed and quantified with a gas micro-chromatograph (Agilent Technologies) and a NH_3/NO/NO_2/N_2O continuous analyzer (ABB, model Advance Optima AO2020). The estimated uncertainty of the measurements is within ± 5%, but not less than 5 ppm for the continuous analysers and 10 ppm for the gas micro-chromatograph, which are the detection limits. Mixtures are diluted in argon because this allows to analyze the formation of N_2 and, thus, to perform nitrogen balances, as will be shown later.

Table 1 summarizes the experimental initial conditions. The influence of pressure at different temperatures has been evaluated in the 10 to 40 bar range for stoichiometries of 1 and 3 (sets 1–6 and 8–9 in Table 1). For the highest pressure studied, 40 bar, we have also considered a fuel-rich stoichiometry of 0.7 (set 7 in Table 1), since the experimental high pressure conditions allowed us to see reaction at comparatively lower temperatures. Set 2R corresponds to a repetition experiment. The experimental results of set 2 and 2R will be later compared in order to evaluate the repetitiveness of experimental results.

3. Kinetic modeling

The experimental results of the present work are simulated using a kinetic mechanism based on earlier work on nitrogen chemistry by Glarborg et al. [11], updated with the recent work of Klippenstein et al. [39], and drawing on more recent work on amine chemistry by Stagni et al. [17], Marshall et al. [40], Alzueta et al. [19,41,42], Glarborg et al. [43,44], Petty et al. [45]. Important changes include the reactions $NH_2 + HO_2$ (Klippenstein et al., [46]) and $NH_2 + NO_2$ (Glarborg [47]), as well as steps involved in amine pyrolysis by Glarborg [44]. The thermodynamic data come from the same sources as the kinetic mechanisms used. The full mechanism, which has been used earlier with success [e.g. 42,47], is available as supplementary material.

Calculations have been carried out using the plug-flow reactor (PFR) model of the Chemkin Pro suite [48], using the initial conditions for each experiment, as listed in Table 1, and a "fix gas temperature" type problem, using the nominal reaction temperature at the flat temperature zone. It has to be mentioned that similar results were obtained with and without the measured temperature profiles.

4. Results and discussion

In order to evaluate the influence of oxygen excess ratio on NH_3 oxidation, experiments highly diluted in Ar at different pressures (10–40 bar) and at different temperatures (600 K-1275 K) have been conducted under reducing, stoichiometric and oxidizing conditions (λ = 0.7, λ = 1 and λ = 3). The experimental results are compared with modeling predictions using the kinetic mechanism previously described. In the Figures, symbols denote the experimental data and lines denote simulation results.

Table 1
Matrix of experimental conditions. All experiments are performed in the 600–1275 K temperature interval with a total flow rate of 1000 ml (STP)/min and using Ar as bath gas. The residence time is defined by equation (2).

Set	NH_3 (ppm)	O_2 (ppm)	P (bar)	λ
1	1023	761	10	1.0
2	1019	2143	10	2.9
2R	983	2092	10	2.8
3	1053	745	20	1.0
4	1036	2230	20	3.0
5	1066	778	30	1.0
6	1068	2203	30	2.9
7	982	538	40	0.7
8	1070	765	40	1.0
9	1039	2265	40	3.0

Fig. 3 shows the results for NH_3 oxidation at the different pressures studied for stoichiometric conditions (λ = 1). It is seen that increasing pressure, keeping the rest of conditions similar, results in a shift of the conversion of ammonia to lower temperatures. Specifically, it can be observed that while for a pressure of 10 bar, the onset of reaction occurs at approximately 1250 K, for the highest pressure studied, 40 bar, ammonia starts to convert at approximately 1165 K. For any pressure studied, as the temperature increases, the NH_3 concentration is sharply reduced at a given temperature. We are not able to reach in our experimental system the full conversion of ammonia due to limitations of the experimental setup (maximum temperature 1275 K). The only nitrogen products at the outlet of the reaction system are unreacted ammonia and molecular nitrogen. No nitrogen oxides (NO, NO_2 and N_2O) and hydrogen in significant concentrations have been detected under the conditions of Fig. 3.

The model generally reproduces well the trends of ammonia consumption, for the different pressures at the stoichiometric conditions of Fig. 3, and the best agreement between experimental and simulated results is found for the higher pressures. Simulation results overpredict slightly NH_3 conversion as the pressure is decreased below 40 bar, but still the agreement is quite good. Modeling calculations indicate that the full conversion of ammonia is obtained for approximately a similar temperature, of about 1275 K, independently of pressure.

Similar results of Fig. 3, but for an oxygen excess ratio of λ = 3, are shown in Fig. 4, where a comparison of experimental and simulated NH_3 concentration as a function of temperature at 10, 20, 30 and 40 bar is done. Again, even for the higher O_2 excess, no hydrogen or other nitrogen products different from unreacted ammonia or nitrogen are detected in appreciable quantities. As can be observed, at λ = 3, the higher the pressure, the lower the temperature necessary for the NH_3 oxidation onset and further complete conversion of NH_3 to occur, which agrees with the findings obtained at atmospheric pressure and similar conditions (Abián et al., [18]) and those obtained at pressures over 30 bar by Song et al. [15], also in a flow reactor. Conversion of ammonia happens at 20–25 K less under oxidizing conditions compared to the stoichiometric conditions of Fig. 3. Full conversion of NH_3 is only attained, experimentally, at 40 bar for the most oxidizing conditions considered.

The agreement between experimental and calculated results is satisfactory as can be seen in Fig. 4, and calculations predict full conversion of ammonia at approximately 1250 K for any pressure analyzed·NH_3 conversion is very well predicted at 40 bar, and it is slightly over-predicted at lower pressures.

The effect of the oxygen excess ratio on NH_3 conversion is slightly different for the different pressures studied. The decrease in pressure from 40 to 30 bar results in an increase of the ammonia conversion onset temperature of approximately 40 K, and each further decrease of 10 bar produces a shift of 20–25 K to higher temperatures of the onset of reaction, in the case of λ = 1, Fig. 3. In the λ = 3 case, Fig. 4, each 10 bar decrease in pressure produces a shift to higher temperature the onset of ammonia conversion of 25–30 K.

Additionally, Fig. S1 in the supplementary material includes the comparison of experimental and calculated results of O_2 concentration for the different pressures and stoichiometries considered in the present work. The agreement between experimental and calculated O_2 concentrations is pretty good.

It should be taken into account that changing pressure in our experimental system, and procedure, implies the change of the residence time according to equation (2). This has been analysed in earlier works

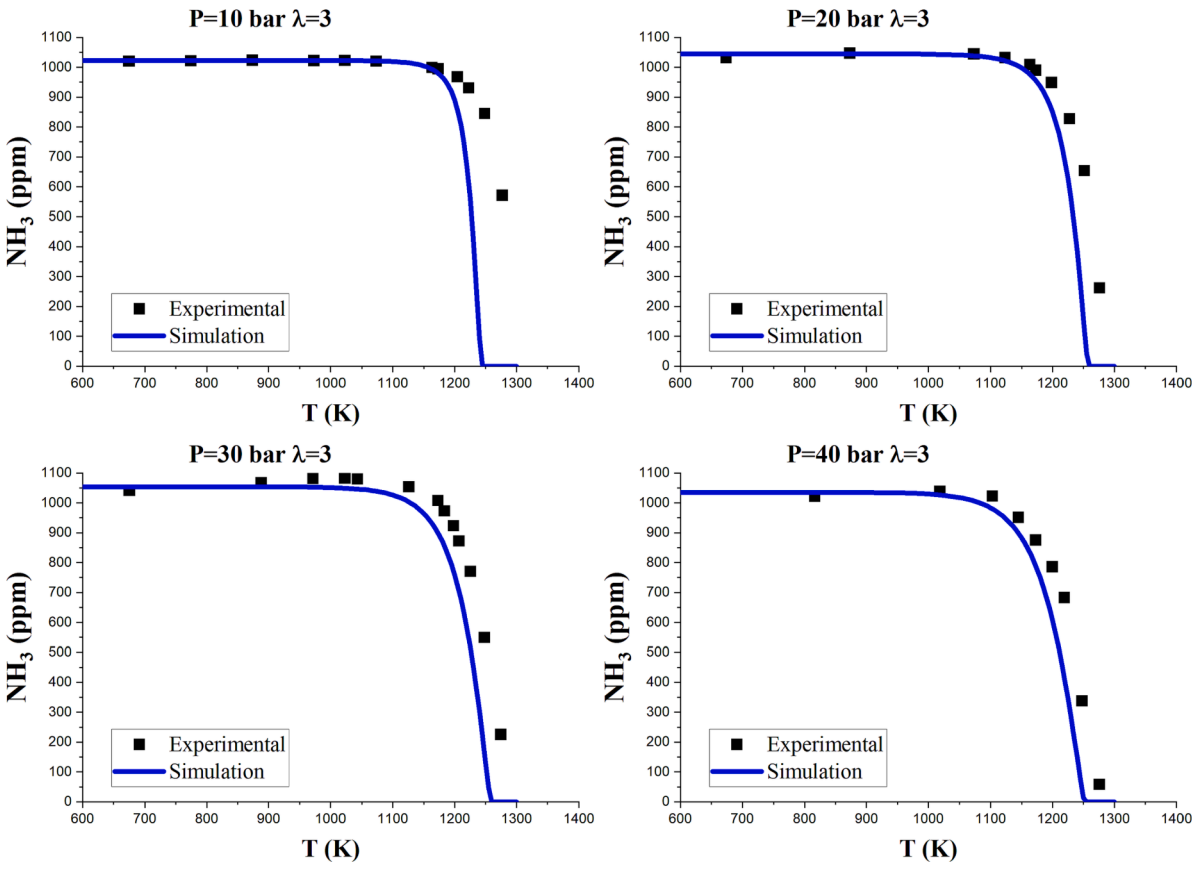

Fig. 3. Comparison of experimental and simulated NH_3 concentration profiles as a function of the reactor temperature at 10, 20, 30 and 40 bar, respectively, and an oxygen excess ratio of $\lambda = 1$ using Ar as bath gas. Experimental conditions correspond to sets 1, 3, 5 and 8 of Table 1.

by our group (see for instance Marrodán et al. [49,50]. Those works indicated that, both, gas residence time and pressure, do have a similar effect on the conversion of species, and that increasing any of them results in a major conversion of reactants at a given temperature. Also, the effect of residence time alone was suggested to be slightly more important than the effect of pressure [49].

Bearing in mind the limitations of the experimental system at high pressure and temperature, we decided to extend the experimental data set as much as possible, and we performed an additional experiment at reducing conditions, $\lambda = 0.7$ (set 7 in Table 1). To do that, we chose the highest pressure studied, 40 bar, since this is the most favourable one in order to reach, if possible, the full conversion of ammonia.

Figs. 5 and 6 compare, respectively, experimental and simulated results of NH_3 and N_2 obtained during the oxidation of NH_3 at different oxygen excess ratio for each pressure studied. Only NH_3 and N_2 are represented because, as mentioned above, those are the only nitrogen products that appear in significant concentrations during the conversion of ammonia under the present experimental conditions. As can be seen, diminishing oxygen concentration shifts the onset of reaction to higher temperatures. Modelling calculations also reflect a similar behaviour, even though the simulated profiles are shifted about 20–40 K to lower temperatures compared to the experimental data. The oxygen concentration is, thus, a key factor in the process, under the high-pressure conditions of the present study, and coinciding with the results of Abián et al. [18] obtained in an atmospheric pressure study of ammonia oxidation similar to the present work. It is worthwhile to mention that, while Abián et al. [18], under similar experimental conditions and atmospheric pressure, obtained NO and NO_2 in small amounts, no formation of these compounds is obtained at high pressure. Actually, no hydrogen or nitrogen species other than N_2 and unreacted NH_3, when present, were found in the different experiments of the present work.

This is a positive outcome of the present results, since emissions of NO, NO_2 and N_2O seem to be limited at high pressures, either because oxidation of ammonia to these products is not favoured, or because in the case of the formation of NO, interaction of it with ammonia through SNCR would be more important at the high pressure conditions at the present work.

Also, it is seen that for $\lambda = 0.7$, the reaction onset of ammonia oxidation is shifted to higher temperatures happening at 1205 K approximately under the conditions of Fig. 5. At the temperature of 1275 K the unreacted NH_3 concentration is 594 ppm at $\lambda = 0.7$, 501 ppm at $\lambda = 1$ and 58 ppm at $\lambda = 3$, which indicates that the higher the oxygen excess ratio, the lower the NH_3 concentrations obtained at a given temperature.

Independently of the stoichiometry, the present results indicate that the increment above 10 bar of pressure (from 10 to 40 bar) does have an effect in the onset of ammonia oxidation reaction. This is different to what observed Song et al. [15] at pressures of 30 and 100 bar, where a similar reaction onset temperature was found, accompanied by the formation of N_2O, which has not been seen in the present experiments. The differences may be attributed to the significantly different stoichiometries and residence time used in the Song et al. work.

Figs. 5 and 6 also show the repeatability of sets 2 and 2R, at 10 bar under oxidizing conditions. As seen, reproducibility of the experiments is very good in all the temperature range considered, which is an indication of the good performance of the experimental system and experimental procedure.

The nitrogen balance for all the experiments made is shown in Fig. 7. The N balance is calculated taking into account the nitrogen atoms of the following species: NH_3, N_2, NO, N_2O, and NO_2. As has been mentioned, only NH_3 and N_2 were detected in appreciable amounts at the reactor outlet, while the different nitrogen oxides, i.e. NO, NO_2 and N_2O, formed

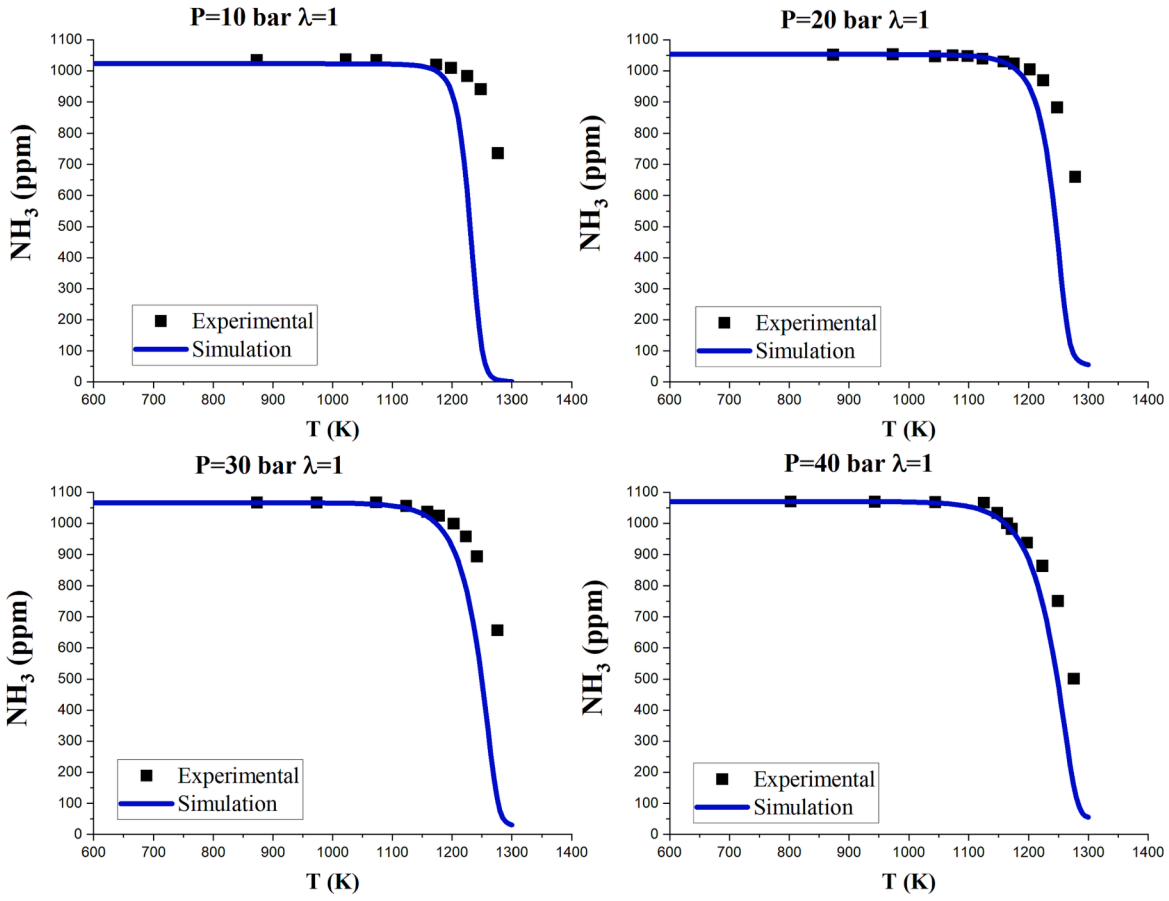

Fig. 4. Comparison of experimental and simulated NH_3 concentration profiles as a function of the reactor temperature at 10, 20, 30 and 40 bar, respectively, and an oxygen excess ratio of $\lambda = 3$ using Ar as bath gas. Experimental conditions correspond to sets 2, 4, 6 and 9 of Table 1.

show concentrations below 5 ppm in any case. Even though these species have been accounted for in the nitrogen balance, their experiment profiles have not been shown in the figures because the concentration of these species is within the uncertainty of the equipment measurements. The N balance (in percentage) calculated with the model of the species mentioned (NH_3, N_2, NO, NO_2 and N_2O) above is also shown in Fig. 7 as a continuous line.

The experimental nitrogen balance closes between 85 and 105 %, while the calculated one closes between 99.9 % and 100 % if all 5 nitrogen species (NH_3, N_2, NO, NO_2 and N_2O) are considered, while it closes between 99 and 100 % if only NH_3 and N_2 are taken into account. This is roughly a further confirmation of the absence of nitrogen products other than ammonia and molecular nitrogen, as experimentally obtained under the conditions of the present work, and different to what was obtained at atmospheric pressure (Abián et al., [18]), or at high pressure (Song et al. [15]) under slightly different operating conditions.

In order to get some insight on the reaction pathway through which the oxidation conversion of ammonia proceeds at high pressure and different stoichiometries, we have made rate of production analyses for the different conditions considered. Fig. 8 shows the results for 10 bar and stoichiometric conditions as an example, even though the main features are similar for all the conditions considered in the present work. The conversion of NH_3 follows a similar evolution than what happens at atmospheric pressure, and the main differences include the more relevant role of the amine chemistry at high pressure, with the NH_2 conversion into N_2H_4 by recombination of these radicals, which is recycled back to NH_2 or reacts with the O/H radical pool.

Calculations indicate that ammonia conversion follows a main pathway going through NH_2. The initiation of the reaction mechanism is described by reactions R(1) and R(2).

$$NH_3 + OH \rightleftharpoons NH_2 + H_2O \quad \text{R1}$$

$$NH_3 + O \rightleftharpoons NH_2 + OH \quad \text{R2}$$

NH_2 is subsequently converted into N_2 and H_2O by reaction R(3), but also through reactions R(4) to R(7) producing NNH and N_2H_4, H_2NO and NH.

$$NH_2 + NO \rightleftharpoons N_2 + H_2O \quad \text{R3}$$

$$NH_2 + NO \rightleftharpoons NNH + OH \quad \text{R4}$$

$$2\,NH_2\,(+M) \rightleftharpoons N_2H_4\,(+M) \quad \text{R5}$$

$$NH_2 + HO_2 \rightleftharpoons H_2NO + OH \quad \text{R6}$$

$$NH_2 + M \rightleftharpoons NH + H + M \quad \text{R7}$$

Finally, the main reactions of N_2 formation are R3 and R8, which also produces hydrogen radicals,

$$NNH \rightleftharpoons N_2 + H \quad \text{R8}$$

As has been mentioned, no appreciable concentration of NO at the outlet of the reactor has been detected in the present experiments, with only NH_3 and N_2 as the nitrogen containing products detected in appreciable concentration. Calculations indicate that the small amount of NO, formed via HNO, quickly reacts through reactions R(3) and R(4), and in a minor extent through reactions (R9) and (R10):

$$NO + HO_2 \rightleftharpoons NO_2 + OH \quad \text{R9}$$

$$NO + HO_2 \rightleftharpoons HNO + O_2 \quad \text{R10}$$

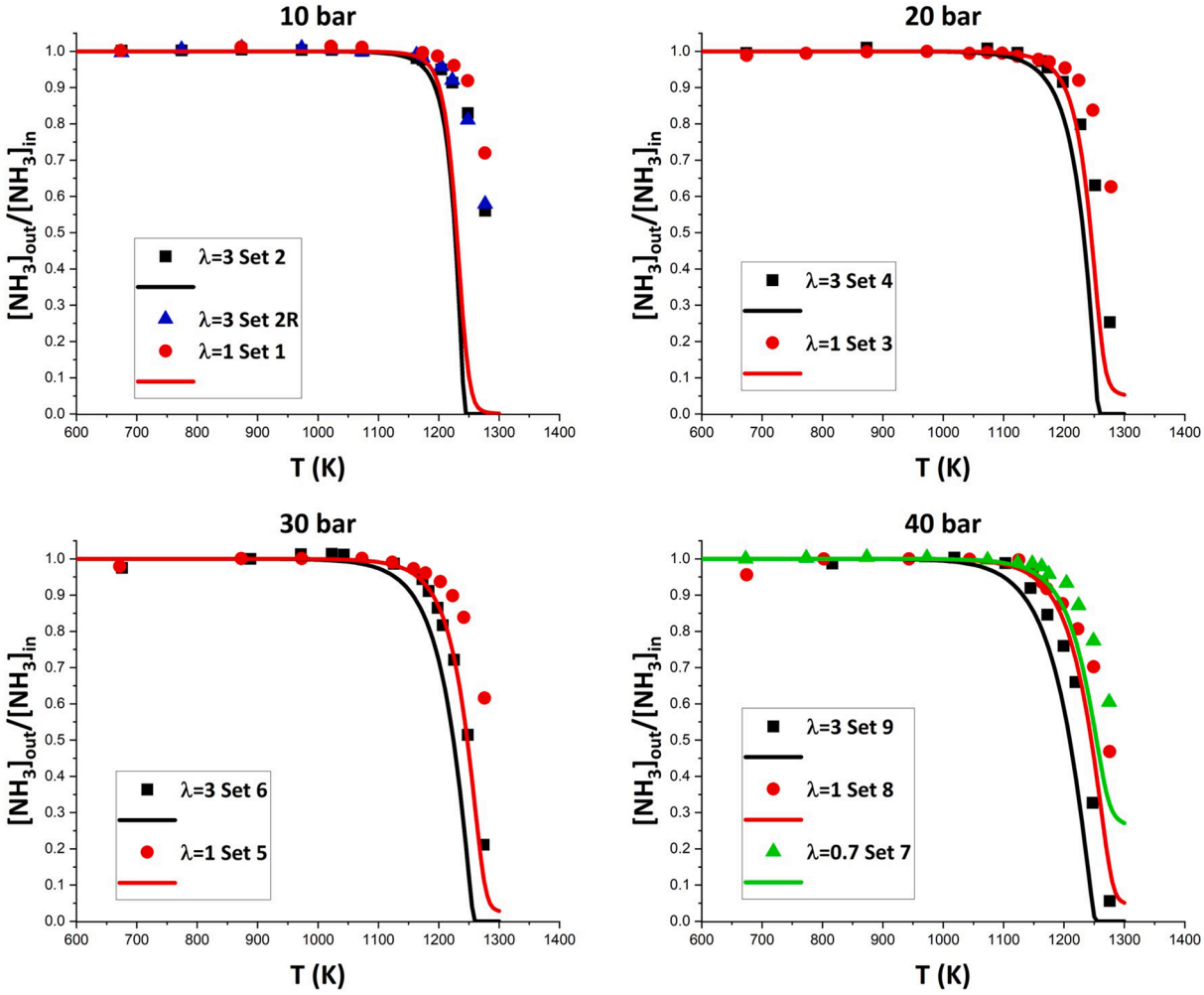

Fig. 5. Comparison of experimental and simulated normalized NH_3 concentration profiles during ammonia oxidation as a function of the temperature and for different oxygen excess ratios: λ = 0.7, 1 and 3, and different pressures: 10, 20, 30 and 40 bar, using Ar as bath gas. Inlet composition is summarized in Table 1, sets 1–9.

R9 is responsible of the presence of negligible amounts of NO_2 (less than 5 ppm) at the outlet of the reaction system. This is consistent with the general knowledge of NO_x chemistry, since at the highest temperatures considered, presence of NO_2 is not feasible since NO is the thermodynamic stable form at the high temperatures of this work.

N_2O has not been detected in significant amounts in experiments, but neither in calculations. The model simulations indicated that the N_2O concentration is very low under the studied conditions, and it is produced from the interaction of NH_2 radicals with the formed NO_2, which is very low, through reaction R11, and effectively decomposed through reaction R12.

$$NH_2 + NO_2 \rightleftharpoons N_2O + H_2O \quad \text{R11}$$

$$N_2O\,(+M) \rightleftharpoons N_2 + O\,(+M) \quad \text{R12}$$

It is clear that under the conditions of the present work the dominant path for ammonia conversion leads to N_2 in any case. Calculations show two main reaction pathways: $NH_3 \rightarrow NH_2 \rightarrow NNH/H_2NN \rightarrow N_2$, and $NH_3 \rightarrow NH_2 \rightarrow H_2NO/NH \rightarrow HNO \rightarrow NO \rightarrow N_2$ in a minor extent, in line with results of previous works [18,19].

While the interaction of ammonia and NO has been considered in the past [e.g. 12,19–21,26], to our knowledge, no study so far has dealt with the interaction of NH_3 and NO occurring at high pressure.

Therefore, experiments of ammonia conversion in the presence of NO were performed in order to evaluate the possible contribution of NO to the oxidation of ammonia at high pressures, since NO can be formed during NH_3 oxidation. Also, ammonia may interact with NO and reduce it through SNCR reactions. Table 2 summarizes the conditions of the experiments performed in the presence of approximately 500 ppm of NO.

As seen, the temperature interval in which the experiments were run is different, and the main reason is that operational problems occurred in those experiments. Thus, the temperatures ranged reported correspond to the interval in which the experiment was run. While running the experiments of Table 2, NH_3 and NO were found to disappear and no formation of N products (i.e. NO_2, N_2O) was observed. Also, the nitrogen balance did not close. The decrease in both NH_3 and NO was accompanied, in all cases, by the sudden formation of a white powder which was found to deposit on the reactor walls and pipes. We analysed this white powder using an elemental analysis equipment (LECO TruSpec® Micro Elemental Analyser) and its composition resulted to be compatible with the formula of ammonium nitrate. Formation of the above mentioned solid was found in all four experiments of Table 2, and was more significant as pressure increased.

We had to stop the present experiments because of operational reasons, but further study of the specific conditions that lead to the formation of NH_4NO_3 at high pressure would be of interest. The formation of solid deposits may imply operational problems in real practical applications. Additionally, ammonium nitrate is a significantly reactive compound, which may also imply undesired operational issues.

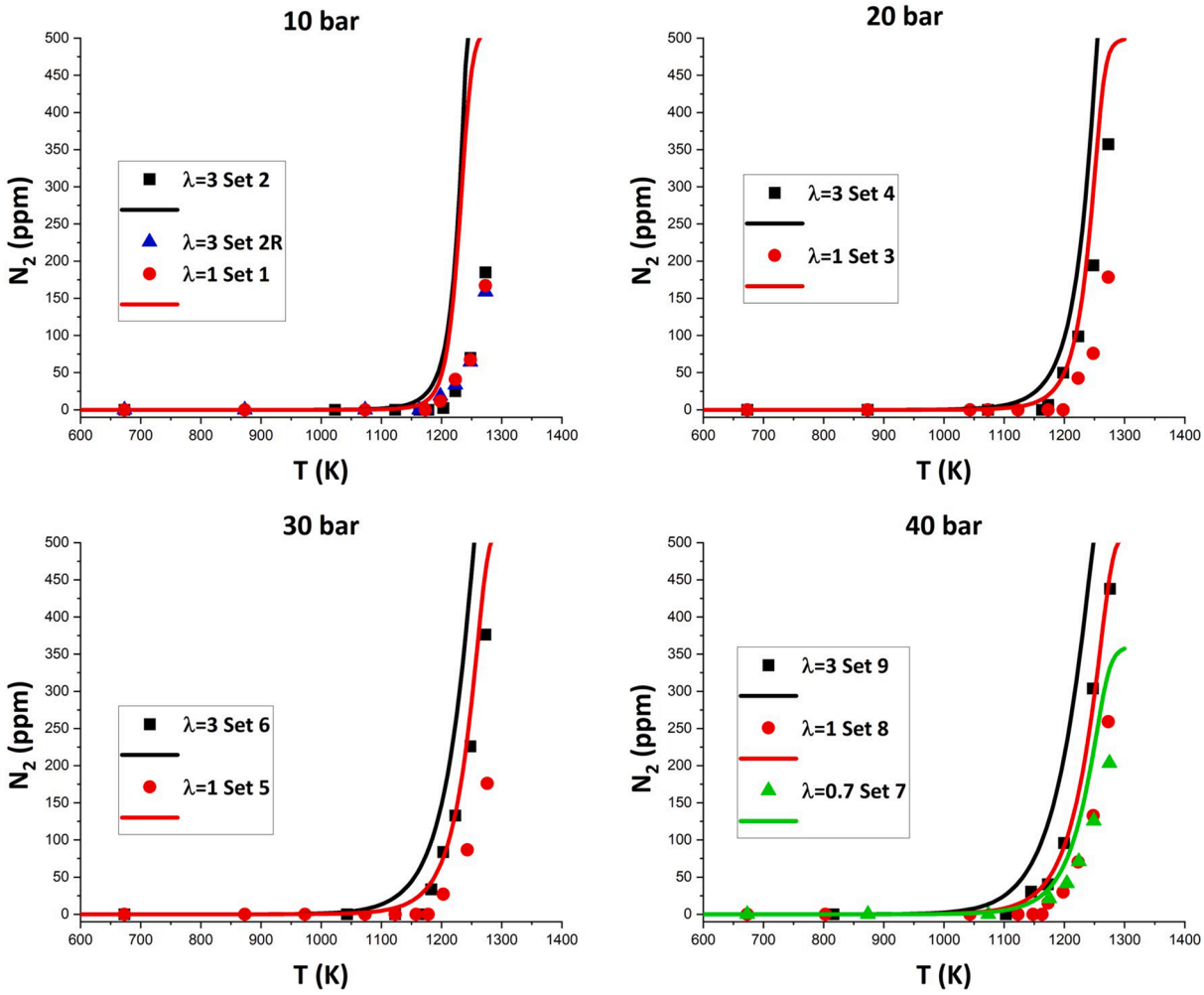

Fig. 6. Comparison of experimental and simulated N_2 concentration profiles during ammonia oxidation as a function of the temperature and for different oxygen excess ratios: λ = 0.7, 1 and 3, and different pressures: 10, 20, 30 and 40 bar, using Ar as bath gas. Inlet composition is summarized in Table 1, sets 1–9.

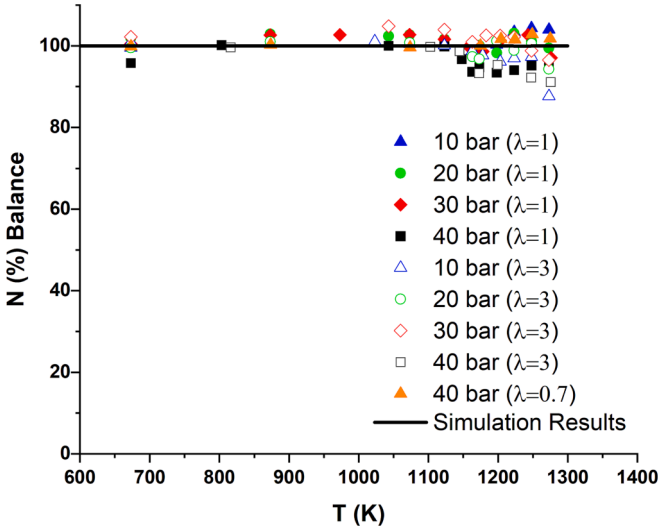

Fig. 7. Experimental and simulated N balance during the oxidation of NH_3, as a function of the reactor temperature, for different oxygen excess ratios and pressures. Sets 1–9 of Table 1.

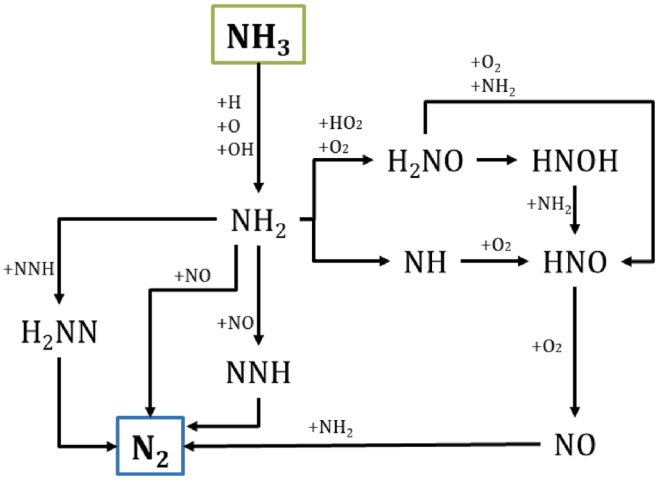

Fig. 8. Reaction path diagram for the oxidation of NH_3 under stoichiometric conditions (λ = 1), and 10 bar of pressure in a quartz flow reactor.

5. Conclusions

An experimental and simulation study of the main features of ammonia oxidation at high pressure (from 10 to 40 bar), under reducing,

Table 2
Matrix of experimental conditions of NH_3 oxidation in the presence of NO. All experiments are performed with a total flow rate of 1000 ml (STP)/min and using Ar as bath gas. The residence time is defined by equation (2).

Set	NH_3 (ppm)	NO (ppm)	O_2 (ppm)	P (bar)	λ	T (K)
10	1037	507	2227	10	2.9	308–1223
11	1037	507	2227	20	2.9	308
12	1004	520	2306	30	3.1	288
13	1004	520	2306	40	3.1	288–1223

stoichiometric and oxidizing conditions in the 600–1275 K temperature interval, in a quartz tubular flow reactor with, roughly, 1000 ppm of inlet ammonia and using argon as diluent, has been performed.

The main product of ammonia conversion is N_2, while H_2, NO, NO_2 and N_2O concentrations are negligible under all conditions studied. The use of high pressure acts to favour the formation of N_2 from ammonia oxidation compared to what happens at atmospheric pressure, for a given temperature. This is a positive outcome for the use of ammonia as a fuel in pressure applications, such as turbines.

The onset of ammonia oxidation occurs at higher temperatures for reducing and stoichiometric conditions than under oxidizing conditions, for all the pressures considered, indicating the importance of oxygen stoichiometry for ammonia conversion. Pressure is seen to have an important influence on the ammonia oxidation regime, shifting it to lower temperatures as pressure increases. However, the influence of pressure is found to be significantly more important at low pressures, compared to the high ones, and the shift to lower temperatures observed for ammonia conversion is higher when changing pressure from 10 to 20 bar than from 30 to 40 bar.

Presence of NO during the conversion of ammonia at high pressure results in the decrease of both NH_3 and NO accompanied by the formation of a white crystalline powder which elemental composition is compatible with the formula of ammonium nitrate.

The mechanism used to carry out the simulations is able to describe the main trends of NH_3 conversion under the conditions of the present work, with a quite satisfactory agreement between experimental and modelling results, even though it overpredicts slightly NH_3 conversion at higher temperatures. The agreement is better for oxidizing conditions.

CRediT authorship contribution statement

P. Garcia-Ruiz: Investigation, Methodology, Writing – original draft, Writing – review & editing. **M. Uruén:** Investigation, Methodology. **M. Abián:** Conceptualization, Methodology. **M.U. Alzueta:** Conceptualization, Formal analysis, Supervision, Writing – review & editing.

Declaration of Competing Interest

The authors declare that they have no known competing financial interests or personal relationships that could have appeared to influence the work reported in this paper.

Data availability

Data will be made available on request.

Acknowledgements

The authors acknowledge the funding from the Aragón Government (Ref. T22_17R), co-funded by FEDER 2014-2020 “Construyendo Europa desde Aragón “, to MINECO and FEDER (Project RTI2018-098856-B-I00 and PID2021-124032OB-I00), and MINECO PRE2019-090162 for financial support.

Appendix A. Supplementary data

Supplementary data to this article can be found online at https://doi.org/10.1016/j.fuel.2023.128302.

References

[1] Mashruk S, Zitouni SE, Brequigny P, Mounaim-Rousselle C, Valera-Medina A. Combustion performances of premixed ammonia/hydrogen/air laminar and swirling flames for a wide range of equivalence ratios. Int J Hydrogen Energy 2022;47(97):41170–82.
[2] Lan R, Irvine JTS, Tao S. Ammonia and related chemicals as potential indirect hydrogen storage materials. Int J Hydrogen Energy 2012;37(2):1482–94.
[3] Wang W, Herreros JM, Tsolakis A, York APE. Ammonia as hydrogen carrier for transportation; Investigation of the ammonia exhaust gas fuel reforming. Int J Hydrogen Energy 2013;38(23):9907–17.
[4] Kobayashi H, Hayakawa A, Somarathne KDKA, Okafor EC. Science and technology of ammonia combustion. Proc Combust Inst 2019;37:109–33.
[5] Philibert C. Renewable Energy for Industry. From green energy to green materials and fuels. International Energy Agency. Paris: 2017.
[6] Valera-Medina A, Amer-Hatem F, Azad AK, Dedoussi IC, de Joannon M, Fernandes RX, et al. Review on ammonia as a potential fuel: From synthesis to economics. Energy Fuels 2021;35(9):6964–7029.
[7] Duynslaegher C, Jeanmart H, Vandooren J. Kinetics in ammonia-containing premixed flames and a preliminary investigation of their use as fuel in spark ignition engines. Combust Sci Technol 2009;181:1092–106.
[8] Otomo J, Koshi M, Mitsumori T, Iwasaki H, Yamada K. Chemical kinetic modeling of ammonia oxidation with improved reaction mechanism for ammonia/air and ammonia/hydrogen/air combustion. Int J Hydrogen Energy 2018;43(5):3004–14.
[9] Oliva M, Alzueta MU, Millera Á, Bilbao R. Theoretical study of the influence of mixing in the SNCR process. Comparison with pilot scale data. Chem Eng Sci 2000;55:5321–32.
[10] Miller JA, Bowman CT. Mechanism and modeling of nitrogen chemistry in combustion. Combust Flame 1989;84:181–96.
[11] Glarborg P, Miller JA, Ruscic B, Klippenstein SJ. Modeling nitrogen chemistry in combustion. Prog Energy Combust Sci 2018;67:31–68.
[12] Shrestha KP, Seidel L, Zeuch T, Mauss F. Detailed kinetic mechanism for the oxidation of ammonia including the formation and reduction of nitrogen oxides. Energy Fuels 2018;32(10):10202–17.
[13] Skreiberg Ø, Kilpinen P, Glarborg P. Ammonia chemistry below 1400 K under fuel-rich conditions in a flow reactor. Combust Flame 2004;136:501–18.
[14] Mendiara T, Glarborg P. Ammonia chemistry in oxy-fuel combustion of methane. Combust Flame 2009;156(10):1937–49.
[15] Song Y, Hashemi H, Christensen JM, Zou C, Marshall P, Glarborg P. Ammonia oxidation at high pressure and intermediate temperatures. Fuel 2016;181:358–65.
[16] Manna MV, Sabia P, Ragucci R, de Joannon M. Oxidation and pyrolysis of ammonia mixtures in model reactors. Fuel 2020;264:116768.
[17] Stagni A, Cavallotti C, Arunthanayothin S, Song Y, Herbinet O, Battin-Leclerc F, et al. An experimental, theoretical and kinetic-modeling study of the gas-phase oxidation of ammonia. React Chem Eng 2020;5:696–711.
[18] Abián M, Benés M, Goñi Ad, Muñoz B, Alzueta MU. Study of the oxidation of ammonia in a flow reactor. Experiments and kinetic modeling simulation Fuel 2021;300:120979.
[19] Alzueta MU, Ara L, Mercader VD, Delogu M, Bilbao R. Interaction of NH_3 and NO under combustion conditions. Experimental flow reactor study and kinetic modeling simulation. Combust Flame 2022;235:111691.
[20] Dagaut P. On the oxidation of ammonia and mutual sensitization of the oxidation of NO and ammonia. Experimental and kinetic modeling. Combust Sci Technol 2022;194:117–29.
[21] Mathieu O, Petersen EL. Experimental and modeling study on the high-temperature oxidation of Ammonia and related NO_x chemistry. Combust Flame 2015;162(3):554–70.
[22] Pochet M, Dias V, Moreau B, Foucher F, Jeanmart H, Contino F. Experimental and numerical study, under LTC conditions, of ammonia ignition delay with and without hydrogen addition. Proc Combust Inst 2019;37:621–9.
[23] Shu B, Vallabhuni SK, He X, Issayev G, Moshammer K, Farooq A, et al. A shock tube and modeling study on the autoignition properties of ammonia at intermediate temperatures. Proc Combust Inst 2019;37:205–11.
[24] Duynslaegher C, Jeanmart H, Vandooren J. Flame structure studies of premixed ammonia/hydrogen/oxygen/argon flames: experimental and numerical investigation. Proc Combust Inst 2009;32:1277–84.
[25] Tian Z, Li Y, Zhang L, Glarborg P, Qi F. An experimental and kinetic modeling study of premixed $NH_3/CH_4/O_2$/Ar flames at low pressure. Combust Flame 2009;156(7):1413–26.
[26] Hayakawa A, Goto T, Mimoto R, Kudo T, Kobayashi H. NO formation/reduction mechanisms of ammonia/air premixed flames at various equivalence ratios and pressures. Mech Eng J 2015;2:14–00402.
[27] Hayakawa A, Goto T, Mimoto R, Arakawa Y, Kudo T, Kobayashi H. Laminar burning velocity and Markstein length of ammonia/air premixed flames at various pressures. Fuel 2015;159:98–106.
[28] Okafor EC, Naito Y, Colson S, Ichikawa A, Kudo T, Hayakawa A, et al. Experimental and numerical study of the laminar burning velocity of CH_4–NH_3–air premixed flames. Combust Flame 2018;187:185–98.

[29] Han X, Wang Z, Costa M, Sun Z, He Y, Cen K. Experimental and kinetic modeling study of laminar burning velocities of NH_3/air, NH_3/H_2/air, NH_3/CO/air and NH_3/CH_4/air premixed flames. Combust Flame 2019;206:214–26.
[30] Zhi Jin B, Deng YF, Xiu Li G, Meng LH. Experimental and numerical study of the laminar burning velocity of NH_3/H_2/air premixed flames at elevated pressure and temperature. Int J Hydrogen Energy 2022;47:36046–57.
[31] Xiao H, Valera-Medina A, Marsh R, Bowen PJ. Numerical study assessing various ammonia/methane reaction models for use under gas turbine conditions. Fuel 2017;196:344–51.
[32] Førby N, Thomsen TB, Cordtz RF, Bræstrup F, Schramm J. Ignition and combustion study of premixed ammonia using GDI pilot injection in CI engine. Fuel 2023;331:125768.
[33] Zhang H, Li G, Long Y, Zhang Z, Wei W, Zhou M, et al. Numerical study on combustion and emission characteristics of a spark-ignition ammonia engine added with hydrogen-rich gas from exhaust-fuel reforming. Fuel 2023;332:125939.
[34] Dai L, Gersen S, Glarborg P, Levinsky H, Mokhov A. Experimental and numerical analysis of the autoignition behavior of NH_3 and NH_3/H_2 mixtures at high pressure. Combust Flame 2020;215:134–44.
[35] Dai L, Hashemi H, Glarborg P, Gersen S, Marshall P, Mokhov A, et al. Ignition delay times of NH_3/DME blends at high pressure and low DME fraction: RCM experiments and simulations. Combust Flame 2021;227:120–34.
[36] Dai L, Gersen S, Glarborg P, Mokhov A, Levinsky H. Autoignition studies of NH_3/CH_4 mixtures at high pressure. Combust Flame 2020;218:19–26.
[37] Marrodán L, Royo E, Millera Á, Bilbao R, Alzueta MU. High pressure oxidation of dimethoxymethane. Energy Fuels 2015;29(5):3507–17.
[38] Colom-Díaz JM, Abián M, Millera Á, Bilbao R, Alzueta MU. Influence of pressure on H_2S oxidation. Experiments and kinetic modeling. Fuel 2019;258:116145.
[39] Klippenstein SJ, Sivaramakrishnan R, Burke U, Somers KP, Curran HJ, Cai L, et al. HO_2 + HO_2: High level theory and the role of singlet channels. Combust Flame 2022;243:111975.
[40] Marshall P, Rawling G, Glarborg P. New reactions of diazene and related species for modelling combustion of amine fuels. Mol Phys 2021;119:1–28.
[41] Alzueta MU, Giménez-López J, Mercader VD, Bilbao R. Conversion of NH_3 and NH_3-NO mixtures in a CO_2 atmosphere. A parametric study. Fuel 2022;327:125133.
[42] Alzueta MU, Salas I, Hashemi H, Glarborg P. CO assisted NH_3 oxidation. Combust. Flame 2023; In press 2023: doi: 10.1016/j.combustflame.2022.112438.
[43] Glarborg P, Hashemi H, Cheskis S, Jasper AW. On the rate constant for NH_2+HO_2 and third-body collision efficiencies for NH_2+H(+M) and NH_2+NH_2(+M). J Phys Chem A 2021;125:1505–16.
[44] Glarborg P, Hashemi H, Marshall P. Challenges in Kinetic modeling of ammonia pyrolysis. Fuel Commun 2022;10:100049.
[45] Petty JT, Harrison JA, Moore CB. Reactions of trans-hydroxy carbonyl radical studied by infrared spectroscopy. J Phys Chem 1993;97:11194–8.
[46] Klippenstein SJ, Glarborg P. Theoretical kinetics predictions for NH_2 + HO_2. Combust Flame 2022;236:111787.
[47] Glarborg P. The NH_3/NO_2/O_2 system: Constraining key steps in ammonia ignition and N_2O formation. Combust. Flame 2022; In press 2022. doi: 10.1016/j.combustflame.2022.112311.
[48] Ansys Chemkin-Pro 18. ANSYS Inc. 2016.
[49] Marrodán L, Arnal AJ, Millera Á, Bilbao R, Alzueta MU. The inhibiting effect of NO addition on dimethyl ether high-pressure oxidation. Combust Flame 2018;197:1–10.
[50] Marrodán L, Millera Á, Bilbao R, Alzueta MU. An experimental and modeling study of acetylene-dimethyl ether mixtures oxidation at high-pressure. Fuel 2022;327:125143.